Comparison of transformer models for switching operations in long step-out cable systems

J. Kolb, H. K. Høidalen

***Abstract* – Transmission systems with long step-out cables are characterized by low frequency parallel resonances. Transformer energization in such systems introduces a significant risk of resonant overvoltages and severe voltage distortions, caused by harmonic currents exciting these resonances. To mitigate these risks, limiting inrush currents during energization is important. This paper investigates the energization and de-energization transients of a subsea power system with a 100 km long 220 kV step-out cable and a 400 MVA 220/66 kV subsea transformer. The switching operations at the 220 kV level are based on onshore circuit breakers at the onshore substation. Transient voltages, currents, and the magnetic flux in the subsea transformer are analyzed and reported. Different transformer saturation and hysteresis models in ATP-EMTP, PowerFactory and PSCAD are compared in the analysis. The model behavior across the various tools is evaluated and the importance of model input parameters is discussed. Uncontrolled and controlled switching strategies are considered and evaluated regarding transformer saturation and resonant overvoltages and power quality distortion.**

***Keywords*: Transformer, inrush current, ringdown transient, residual flux, hysteresis, offshore wind.**

I. Introduction

Recent developments in transmission system technologies for offshore wind energy projects and the electrification of remote offshore island grids have resulted in new challenges associated with the energization of transformers. There are many offshore wind and electrification projects currently being developed where the offshore transmission system is characterized by long step-out cable connections from the onshore grid. The length for HVAC cable connections have increased significantly over the past few years and include various projects where the step out length exceeds 200 km with operational voltages between 110 kV and 230 kV.

In addition to increasing lengths for the HVAC transmission links, subsea equipment is currently being introduced in some projects. The primary motivation for this shift is to replace traditional offshore platforms with topside equipment with subsea substations, significantly reducing the civil costs associated with the offshore infrastructure. Subsea transformers are used in these offshore substations and connected directly to the HVAC sea cable by dry-mate connectors. Switching operations for the subsea cable and transformer are carried out with the onshore circuit breaker. The subsea transformer is therefore energized simultaneous with the subsea cable from the onshore substation. Fig. 1 shows an example for a typical floating offshore wind project with subsea transformer and a long step-out cable to the onshore substation.

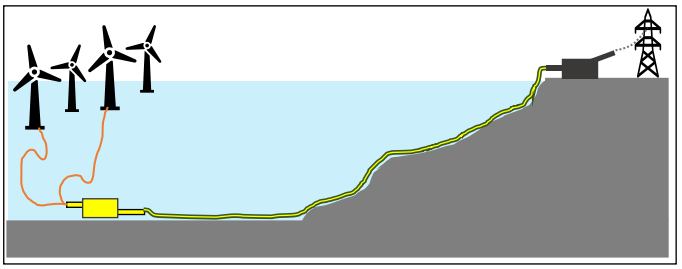

Fig. 1: Illustration of an example 220 kV offshore transmission system floating offshore wind with long step-out subsea cable and subsea transformer

Offshore transmission systems and transients related to the energization of such systems is well studied in literature [1-9]. In [1] the energization of the 55 km cable at Horns Rev is compared with measurements, revealing de-energization as the most difficult case to represent. Temporary overvoltage due to resonance conditions and de-energization due to zero-miss of the current are well studied [4-6]. Low frequency resonance is studied in [3, 8, 9]. High frequency resonance is similarly studied [2, 7, 9]. Zero-miss phenomenon is analyzed in [1, 8]. Inrush currents and mitigation are discussed in [1, 8]. Less reported in literature is energization and de-energization of long cables connected to unloaded transformer where the magnetic core of the transformer is crucial [10, 11], especially in de-energization studies.

Offshore transmission systems with long HVAC cable connections are characterized by low frequency parallel resonances. The energization of transformers give rise to inrush currents containing substantial second and third order harmonic currents. These inrush currents pose a risk for resonant overvoltages and power quality distortion. Inrush currents during energization therefore need to be limited to a minimum.

Controlled point on wave (PoW) switching is traditionally applied to reduce inrush currents and the associated challenges during the system energization. It allows to regulate the PoW for circuit breaker contact touching and thus, the instantaneous voltages in the three-phases during the closing operation.

The accurate prediction of the residual flux in the transformer iron core is essential for effective controlled PoW switching and mitigation of high transformer inrush currents. The residual flux in the transformer depends on the de-

J. Kolb is with Unitech Power Systems as Technical Lead Engineer in Stavanger, Norway (e-mail: Johannes.kolb@unitech.no)
H. K. Høidalen is with the Department of Electric Power Engineering, Norwegian University of Technology (NTNU), Trondheim.
(e-mail: hans.hoidalen@ntnu.no).

Paper submitted to the International Conference on Power Systems Transients (IPST2025) in Guadalajara, Mexico, June 8-12, 2025.

energization transient prior to the energization of the transformer, which depends on the operating conditions prior to disconnection of the transformer, timing of the switching operation (switching angle) and the equipment which is connected to the disconnected transformer. The de-energization of subsea transformers in offshore transmission systems with long cables is followed by a ringdown transients where the flux in the transformer oscillates in a resonant circuit with the sea cable after the disconnection. The ringdown transient in such a system is quite complex and challenging to simulate, as the transformer hysteresis representation is essential for the corresponding phenomena. Furthermore, voltage transformers (VTs) are usually connected to the sea cable side of the onshore circuit breaker and discharge the cable after disconnection. The corresponding discharge transient is expected to discharge also the magnetic flux in the transformer. However, this is not considered here and suggested for future work.

The purpose of the study in this paper is to investigate the energization and de-energization transients for long step-out cables with subsea transformers, using different models across various tools (EMTP-ATP, PowerFactory and PSCAD). The paper discusses differences in the model behavior and the importance of model input parameters for such studies. Furthermore, controlled point on wave switching sequences to mitigate inrush currents are evaluated and presented. The work is based on a real-world offshore wind project but has been generalised to maintain the client confidentiality

II. Power System Model

A. Model Introduction and Simulation Tools

The model used in this paper is shown in Fig. 2 and comprises a 100 km, 220 kV step-out subsea cable and a 400 MVA, 220/66 kV subsea transformer. The network is representative for onshore grid connected floating offshore wind park projects which are currently being developed for various sites around the world. It is represented in ATP-EMTP, PowerFactory and PSCAD. Comparative EMT time domain simulations were carried out for individual components and showed a very good accuracy and capabilities for transformer and cable models across the various tools. The simulation results from the various tools are exported as COMTRADE files and PowerFactory was used as the central tool to synthesize and visualize the results from the various tools.

B. Onshore Grid Source

The floating offshore wind project investigated in this paper is shown in Fig. 2. The system is connected to a 400 kV transmission system by a 450 MVA transformer. The onshore substation includes a STATCOM unit for dynamic reactive power control, along with variable and fixed shunt reactors for steady-state reactive power compensation. For this study, the entire onshore substation is simplified and represented by a Thevenin equivalent at 220 kV, assuming minimum short circuit levels of 2530 MVA, with a X/R ratio of 18, which gives Thevenin equivalent impedance of 0.85+j21 Ω.

Steady-state voltage control is managed by the onshore 400/220 kV transformer, which regulates the offshore 66 kV voltage at the subsea transformer. During energization, the onshore 220 kV voltage is temporarily lowered by the 400/220 kV onshore transformer OLTC to achieve nominal operating at the offshore end of the step-out cable and compensate for the Ferranti effect along the subsea cable. Prior to energization, the corresponding voltage is 189 kV (0.86 pu) and after energization 214 kV (0.97 pu) which gives 220 kV voltage at the subsea transformer primary side.

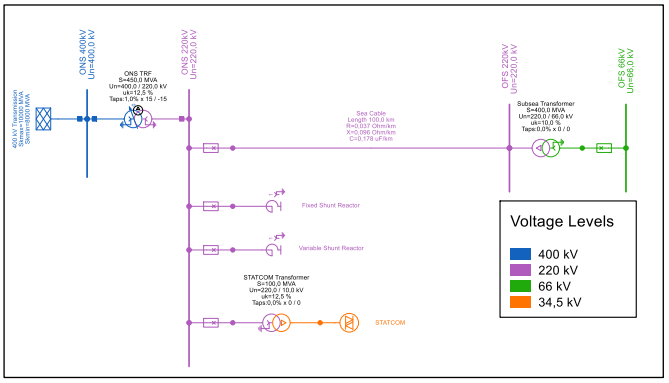

Fig. 2. Overview of a typical 360 MW floating offshore wind park cluster with a 400 MVA 220/66 kV subsea transformer and 100 km subsea cable.

C. Long step-out sea cable

The HVAC offshore transmission link is based on a long step-out sea cable with 1x3x1000mm^2 Cu and U_m=245 kV. The positive and zero sequence impedances for 20°C are documented in Table I. Frequency dependent cable parameters were derived for the corresponding cable using Flux 2D. However, due to the low frequency of the corresponding phenomena, the cable model has a minor impact on the simulation and therefore, a simple Bergeron model was used for the analysis in this paper, as recommended in [4].

TABLE I
SUBSEA CABLE PARAMETERS FOR 50 HZ

Parameter	Positive sequence	Zero sequence	Unit
Resistance	0.037	0.114	Ω/km
Inductance	0.307	0.486	mH/km
Capacitance	0.178	0.178	µF/km
Conductance	0.000	0.000	µS/km

D. Subsea 400 MVA 220/66 kV power transformer

Subsea power transformers are specialized devices designed for deployment on the seabed and engineered to withstand highpressure. The offshore transmission system in this paper includes a 400 MVA subsea transformer. The transformer parameters which are assumed for the work in this paper are documented Table II (additional parameters are confidential).

This analysis considers four distinct transformer models across three different software tools. In ATP-EMTP, the topological Hybrid Transformer Model (XFMR) with Type 96 saturation and hysteresis, as well as the saturable transformer with the Dynamic Hysteresis Model (DHM), which is specifically designed to capture dynamic hysteresis effects, are considered.

TABLE II
SUBSEA TRANSFORMER PARAMETERS

Parameter	Value	Unit
Primary voltage (HV)	220.0	kV
Secondary voltage (LV)	66.0	kV
Rated power	400	MVA
Vector group	Dyn11	-
Short circuit impedance	10.0	%
Copper losses	400	kW
No load current	0.1	%
Eddy current losses	80	kW
Hysteresis losses	80	kW
Air/saturated core reactance	0.2	p.u.
Knee flux	120	%

In PowerFactory, the standard transformer EMT model is utilized, which includes hysteresis functionality. Meanwhile, in PSCAD, the classical transformer model with the basic hysteresis model is used. The models are referred to in this paper as follows:

- Model 1: PowerFactory
- Model 2: ATP-EMTP XFMR
- Model 3: ATP-EMTP DHM
- Model 4: PSCAD

In model 1, the polynomial saturation function (1) is used around the knee point, switching to linear segments at unsaturated and extreme saturation. A factor K=33 was chosen [14]. In model 4, equation (2) is used for the saturation curve [13], where D given by the knee-point parameters. In both cases, the nonlinear inductance is implemented as a current source and placed star point. Model 2 is based on the Frohlich curve given by equation (3) [12]. The characteristic is further discretized in a piecewise linear curve and implemented as a nonlinear inductance.

$$i = \frac{\lambda}{L_m} \cdot \left(1 + \left(\frac{\lambda}{\lambda_0}\right)^K\right) \wedge \lambda_0 = \lambda_{knee} \frac{K+1}{K} \left(\frac{L_m / L_{ac} - 1}{K+1}\right)^{-1/K} \quad (1)$$

$$i = \frac{\sqrt{(\lambda - \lambda_K)^2 + 4D \cdot L_{ac}} + \lambda - \lambda_K}{2L_{ac}} - D/\lambda_K \quad (2)$$

$$\lambda = \frac{i}{a + b|i|} + L_{ac} \cdot i \quad (3)$$

Fig. 3 compares the three magnetization characteristics in pu. Apparently, there are considerable differences in the saturated region where the model 4 is lower. These differences are, however, compensated by the effect of the leakage inductance which is differently included in the models. Models 1, 3 and 4 are set to add half of the leakage inductance to the core model (primary side). Model 2, with the excited winding as the outer, adds 1.5 times the leakage to the core model. This gives the following relation between the total flux inside the excited winding in model 1, 3, 4 on the left side and model 2 on the right side in (4):

$$k_{hl} \cdot L_{leak} + L_{ac} = 1.5 \cdot L_{leak} + k_{ac} \cdot L_{ac} \quad (4)$$

With L_{leak}=0.1 pu, L_{ac}=0.2 pu and the factor k_{hl} set to 0.5, the air-core scaling factor k_{ac} in model 2 also becomes 0.5. It must be noted that more leakage should have been added to models 1, 3 and 4 and k_{hl} set to the maximum value of 1.

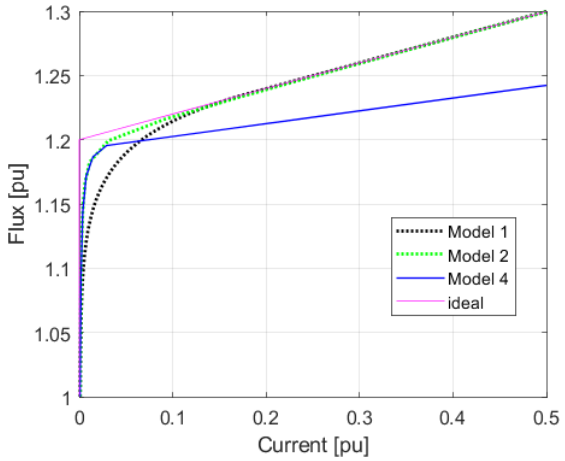

Fig. 3. Saturation curve of the different transformer models

Furthermore, a hysteresis model was defined for all models and a constant loop width was chosen here. The hysteresis model for transformer models 1 and 4 is based on a width-factor which was tuned to obtain 80 kW hysteresis losses during steady state no load operation at nominal voltage, which corresponds to 50% of the total no load losses. The corresponding width factor is 0.0375% for model 1 and 37 for model 4. In model 2, the hysteresis losses can be specified directly with 80 kW and the associated loop width is derived internally. Model 3 [10, 11] is based on the physical core design and uses the input parameters of the core area A, length l, number of turns N and the magnetic material. These are related to nominal and saturated quantities as formulated in (5)-(6).

$$\lambda_{knee} = B_{\max} \cdot A \cdot N \Rightarrow A \cdot N = \frac{\lambda_{knee}[pu]}{B_{\max}(\approx 2T)} \cdot \sqrt{2} U_w \quad (5)$$

$$L_{ac} = \mu_0 N^2 A / l \Rightarrow l = \frac{N^2 A \mu_0}{L_{ac}[H]} \quad (6)$$

One of the parameters A, l or N can be chosen freely and the parameter N=100 was chosen. This gives A=1.029 m^2 and l=1.866m. The material M4 was assumed in this case. No further tuning of the hysteresis or the losses are needed.

Benchmarks for transformer energization with an ideal voltage source were carried out and gave nearly identical results for all models, using the input parameters from Table II.

III. SIMULATION RESULTS

The model described in the previous section is used to simulate the energization, de-energization and re-energization of the subsea transmission system based onshore circuit breaker actions. The simulation time step of 10 µs was chosen, to accurately capture the nonlinear core behavior of the transformer models.

A. Subsea Transmission Energization (Uncontrolled)

In this section, the onshore circuit breaker is operated without being synchronized to the AC voltage waveform, which means that the contacts are closed randomly along any point on

wave of the instantaneous voltage. Pole scatter between the individual single pole circuit breaker units is not considered. A reduced onshore voltage of 0.86 pu is assumed for energization.

First, the energization of the subsea transmission system is analyzed with a single simulation, by closing the 220 kV onshore circuit breaker at t=0.035s (voltage zero-crossing of phase A), with all phases closing simultaneously. The residual flux in the subsea transformer is assumed to be zero. Simulation results are depicted in the Figs. 4-6 and show that the energization causes saturation in the subsea transformer, with magnetizing fluxes reaching 1.66 pu and peak inrush currents reaching 1.34 pu ($\Psi_{base} = 1000 \cdot \frac{U_{Base}}{\sqrt{2} \cdot \pi \cdot f_{nom}} = 990 Vs$; I_{Base}=1485 A_{peak}). The harmonic components in the subsea transformer inrush currents excite the lower order resonance (parallel resonance at approximately 137 Hz) in the system, leading to temporary overvoltages. The maximum overvoltages at the offshore

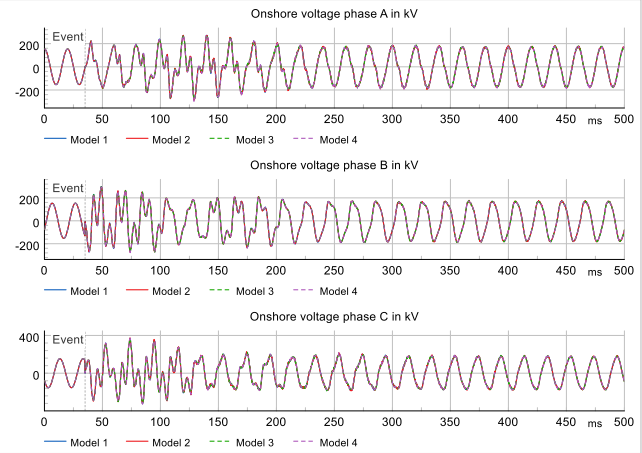

Fig. 4. Onshore substation phase-to-earth voltages in kV.

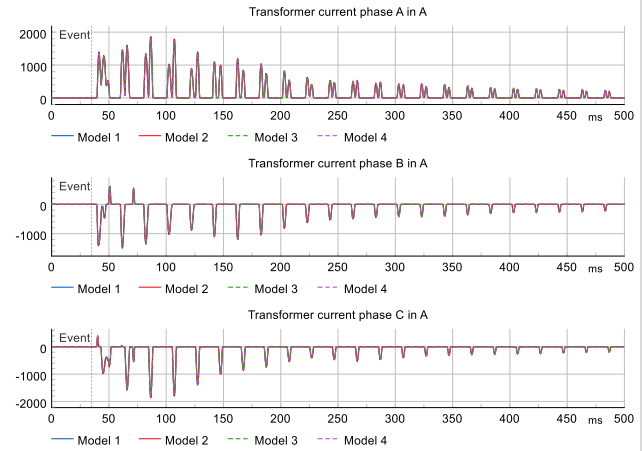

Fig. 5. Subsea transformer primary side phase currents in A.

transformer are 418 kV_{peak} (phase-to-earth) and 710 kV_{peak} (phase-to-phase), while the corresponding maximum onshore voltages are 375 kV_{peak} and 647 kV_{peak} respectively. The simulation results are almost identical with all models and across the different tools, showing that all considered models are well-suited for accurately simulating the energization. The hysteresis is of minor importance for the simulation, while the representation of the air core reactance and saturation curve is the key parameter, in addition to the sea cable model and source representation.

Secondly, 100 multirun simulations are carried out where the circuit breaker closing time is varied for one period (20 ms) in 0.2 ms steps, to account for all relevant circuit breaker closing times. Fig. 7 shows the maximum inrush currents for the multirun analysis. The maximum inrush currents from model 1 range from 1.00 pu to 1.34 pu, with an average peak inrush current of 1.18 pu for all runs. Inrush currents for models 2, 3 and 4 are lower. The maximum peak currents for these models range from 1.22 pu to 1.26 pu, with an average ranging from 1.08 pu to 1.11. All in all, the inrush currents are highest with model 1 and lowest for model 4, while results for models 2 and 3 are between and almost identical for all switching angles.

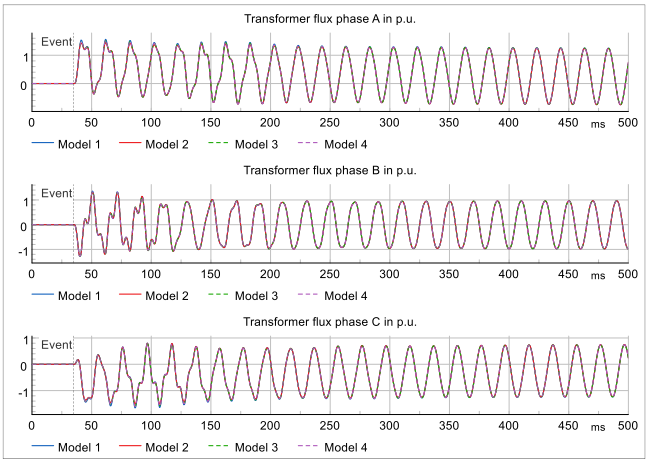

Fig. 6. Subsea transformer magnetic fluxes in pu.

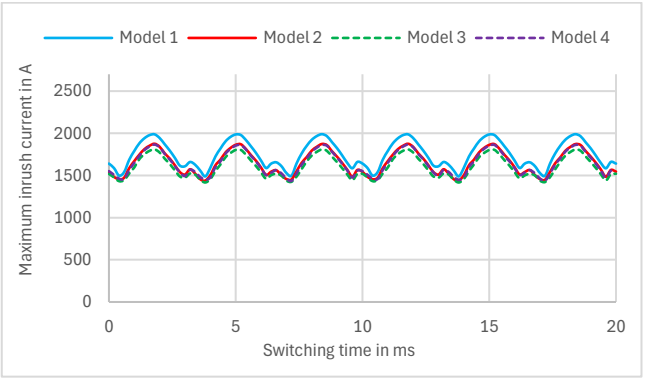

Fig. 7. Peak inrush current with uncontrolled switching sequence

B. Subsea Transmission Energization (Controlled PoW)

The transformer saturation and associated inrush currents and resonant phenomena can be mitigated with controlled PoW switching. Various controlled switching strategies are employed in the industry [15]. Single-phase circuit breakers are usually used for the system studies in this paper. This allows each pole to be switched independently. Assuming that the residual flux in the subsea transformer is zero, the following switching sequence was found to minimize inrush currents for the triplex subsea transformer:

- Event 1: close phase A at voltage peak
- Event 2: close phase C with 3.33 ms (60°) delay
- Event 3: close phase B with 6.66 ms (120°) delay

The energization transients resulting from this switching sequence are shown in Fig. 8-10. The figures show that the inrush currents, along with the associated resonant overvoltages and power quality distortion are effectively reduced and almost completely mitigated. Differences across the various models are negligible and the transformer phase currents remain below 5 A (no load current) during the energization with all models. The overvoltages during the first few periods are associated with the energization of the cable and corresponding travelling wave effects.

The circuit breaker's closing instance (when contacts touch) is associated with some uncertainties and inaccuracies [16], also if controlled switching is applied. As a result, the actual closing time during the PoW sequence usually deviates to some extent from the ideal closing time. In general, the maximum expected inaccuracy of a controlled switching device is ± 2 ms for high voltage circuit breakers [16].

Fig. 11 illustrates the peak inrush current for the above switching sequence for a complete period (20 ms) with 0.2 ms steps. The closing times 0 ms, 10 ms and 20 ms in Fig. 11 correspond to ideal closing times to mitigate transformer saturation and associated inrush currents (phase A at peak voltage, phase B 120° and phase C 60° delayed). The maximum

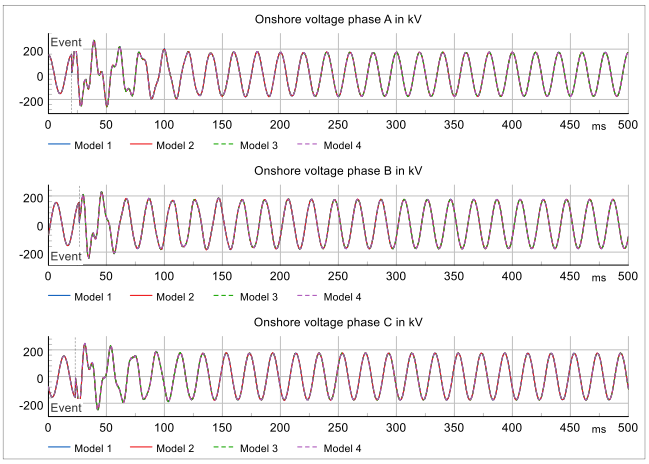

Fig. 8. Onshore substation phase-to-earth voltages in kV.

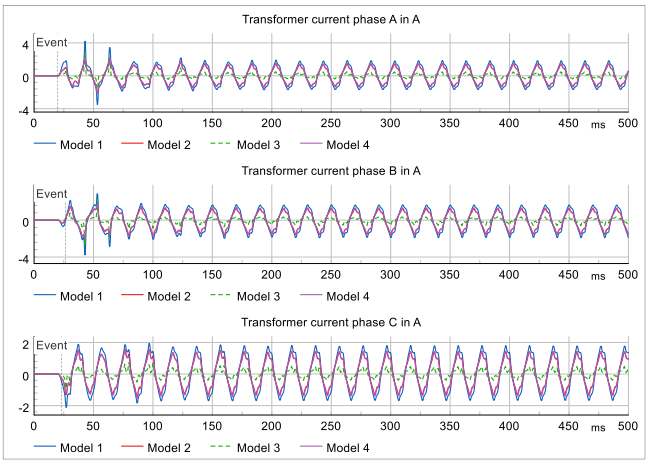

Fig. 9. Subsea transformer primary side phase currents in A.

inrush currents remain below 0.30 pu with all models for ±1.0 ms switching accuracy. For ± 2 ms inaccuracy of the PoW switching sequence, the maximum inrush currents reach approximately 1.0 pu for all models. The maximum inrush currents for all point on waves reaches 1.5 pu, exceeding the 1.3 pu observed with uncontrolled switching. Improper implementation of controlled PoW switching can therefore lead to inrush currents and resonant overvoltages during the energization that are higher than with uncontrolled switching.

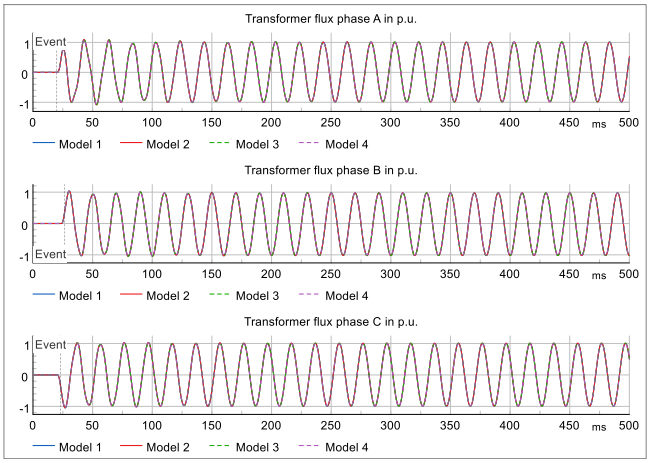

Fig. 10. Subsea transformer magnetic fluxes in pu.

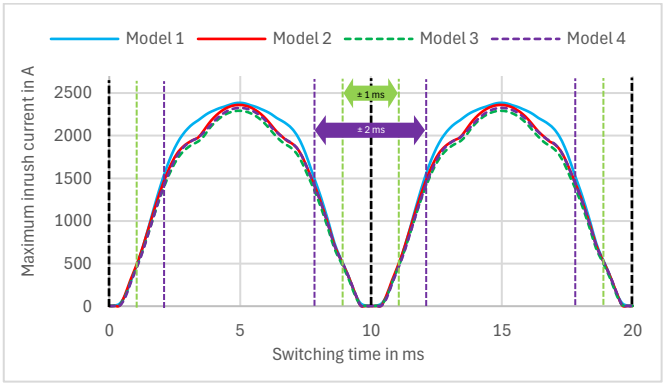

Fig. 11. Peak inrush current with controlled PoW switching

C. *Subsea Transmission De-Energization*

The de-energization of the subsea transmission system is examined by opening the 220 kV onshore circuit breaker at t=0.035s (voltage zero-crossing of phase A). Current interruption occurs at the subsequent current zero-crossing in each phase. Since the steady-state voltage and current on the onshore side of the subsea cable are nearly 90° phase shifted, the current interruption coincides with the peak voltage. Consequently, the sea cable is disconnected with approximately 1 pu voltage, leaving its cable capacitances fully charged. Following the disconnection, the stored energy oscillates between the cable capacitances and the magnetizing impedance of the transformer. The initial system response during the first few fundamental frequency cycles after de-energization is consistent across all considered models in as seen in Figs. 12-14. Following the disconnection, the voltage, current, and magnetic flux exhibit damped oscillations at a subsynchronous frequency, reflecting the transient interaction between the cable capacitance and the magnetizing impedance of the subsea transformer. However, significant differences emerge between

models after a few oscillation cycles. The differences are associated with variations in the hysteresis model and development of the magnetizing flux in the transformer iron core. Since all other parameters have been extensively benchmarked and validated, the differences are associated with the representation of the transformer hysteresis.

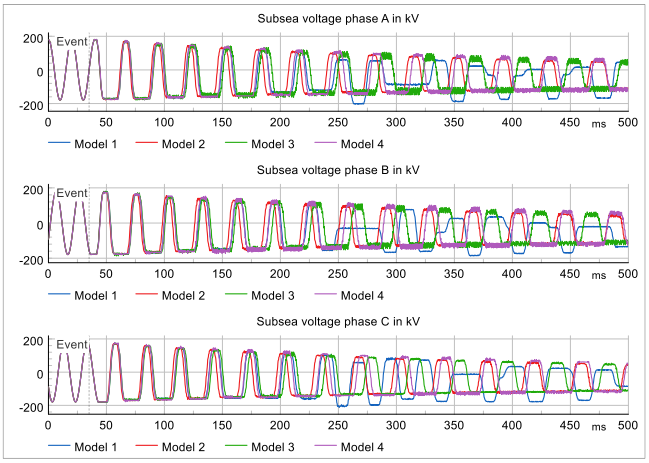

Fig. 12. Offshore subsea phase-to-earth voltages in kV.

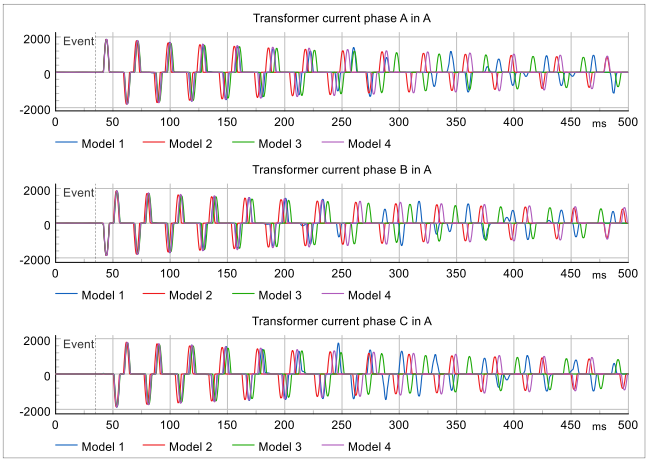

Fig. 13. Subsea transformer primary side phase currents in A.

D. Subsea Transmission Re-Energization

This section investigates the re-energization shortly after the de-energization through a single simulation run based on uncontrolled switching. Initially, the system operates under steady-state conditions before being disconnected at t=0.035s (voltage zero-crossing of phase A) by opening the onshore circuit breaker. Re-energization occurs at t=10 s. The response of the system during re-energization is shown in Figs. 15-17, comparing the results for the different models. According to Fig. 17, only model 3 arrives at a constant flux at 10 s. Model 2 still oscillates at 10 s somewhat and arrives at residual fluxes aperiodic in time and without phase symmetry. The magnetic flux and voltage in the system remains oscillatory for model 1 throughout the 10 s until the onshore circuit breaker re-closes. With model 4, the magnetic flux and voltage arrives at zero.

Re-energization transients vary across the models due to differences in remanent fluxes when the system is re-energized.

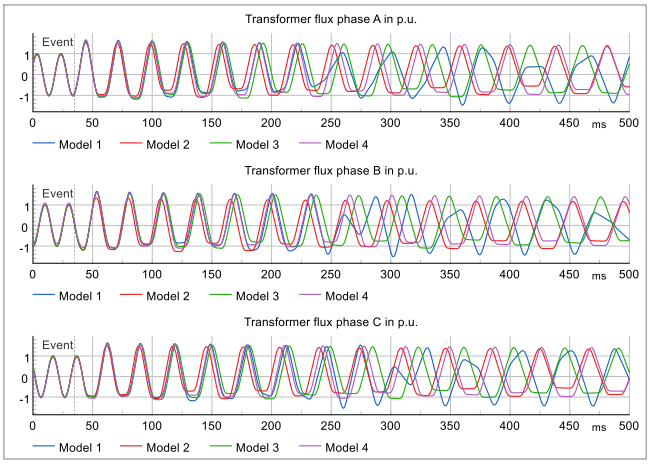

Fig. 14. Subsea transformer magnetic fluxes in pu.

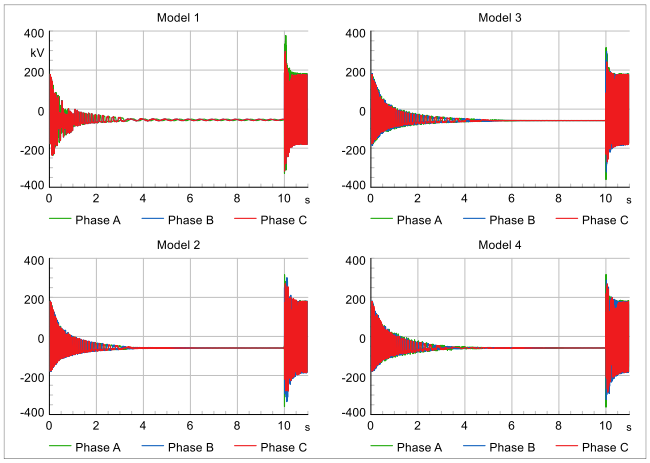

Fig. 15. Offshore subsea phase-to-earth voltages in kV.

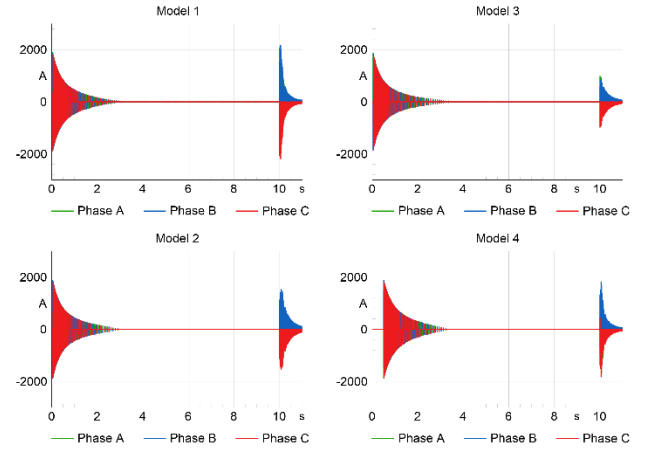

Fig. 16. Subsea transformer primary side phase currents in A.

IV. Discussion

Four different transformer models across three different software tools were considered for the simulation of the energization and de-energization transients of a long cable step-out connected directly to a subsea transformer.

The models show very similar responses for the energization transients and give almost identical voltages, currents and transformer fluxes during the event. The energization of the subsea transmission system results in transformer saturation

with significant inrush currents that excite low order resonances and give rise to serious resonant overvoltages and power quality distortion during the event. Simulations show that the inrush currents can be limited effectively by controlled switching. Switching sequences presented in this paper limit inrush current and the resonant overvoltages effectively, assuming zero residual flux in the subsea transformer prior to energization. This applies also if uncertainties and inaccuracies associated with the ideal point on wave for the controlled switching devices are considered.

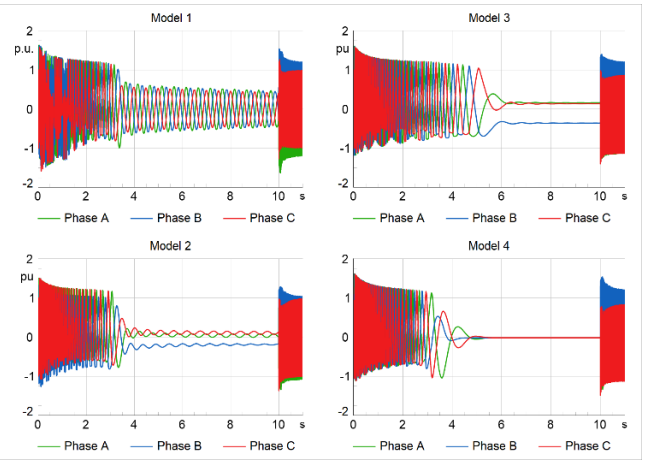

Fig. 17. Subsea transformer magnetic fluxes in pu.

The de-energization of transformers connected to a long step-out cable gives rise to ring-down transients, lasting for several seconds. The outrush current during the de-energization is significant (approximately 1.3 pu). The four models give initially almost identical results, but after some time (approximately 100 ms) the models started to drift apart. In this case the hysteresis model is essential for the correct simulation of the system response. Only model 3 arrives at a steady state residual flux during the simulation, while model 4 arrives at zero residual flux and model 1 remains oscillatory.

Voltage transformers on the sea cable side of the onshore circuit breaker were not included in the model and should be considered in future work, as they are expected to impact de-energization transients. Furthermore, both high- and low frequency transient components are included in the transients, suggesting the use of a broad-band cable model, although the event is dominated by low frequency oscillations. Additionally, the STATCOM at the onshore substation is anticipated to dampen energization transients, with its impact depending on the implemented control strategy and size. Vendor (black-box) models are typically required for such studies and considered once projects reach a mature. In contrast, onshore shunt reactor(s) have a minor impact on simulation results.

V. Conclusion

The energization and de-energization transients were investigated for an offshore wind project with a long HVAC step-out cable connected directly to a subsea transformer. Four different transformer models in ATP-EMTP, PowerFactory and PSCAD were considered in the analysis. The various models show a good agreement for energization transients. Uncontrolled energization gives rise to serious resonant overvoltage and power quality distortion. Maximum inrush currents in the order of 1.3 pu are obtained and peak overvoltages around 700 kV (phase-to-phase) arise for worst case conditions. The air-core inductance and saturation characteristic are the key modelling parameters, in addition to the sea cable and source model. Simulations show that transformer saturation and associated inrush currents and resonant issues can be mitigated effectively with the controlled switching sequence which was proposed in this paper. The sequence is based on single pole circuit breaker operation and closes phase A at its peak and phase B with a 120° delay and phase C with a 60° delay.

De-energization transients show a similar simulation response for all four models during the first few power frequency cycles, however, drift apart approximately 100 ms after the sea cable and subsea transformer are disconnected. The hysteresis model is essential for the simulation of the de-energization transient and only the DHM in ATP-EMTP manages to arrive at consistent residual flux after de-energization with a maximum value of 0.35 pu. The other models either give zero residual flux or continuous oscillating flux.

The use of pre-insertion resistors might be an alternative for controlled PoW switching to mitigate inrush currents, however, was not considered in the paper.

VI. References

[1] F. M. F. da Silva, Analysis and simulation of electromagnetic transients in HVAC cable transmission grids, PhD thesis AAU 2011

[2] I. Arana Aristi: Switching overvoltages in offshore wind power grids, PhD thesis DTU, 2011

[3] S. Deschanvres, Y. Vernay, “Transient Studies performed by RTE for the connection of offshore wind farms”, IPST 2013

[4] Cigre WG C4.502: “Power System Technical Performance Issues Related to the Application of Long HVAC Cables”, TB556, 2013.

[5] Cigre WG C4.307: Transformer Energization in Power Systems: A Study Guide, TB568, 2014

[6] Cigre JWG A2/C4.39: Electrical Transient Interaction Between Transformers and the Power System, TB577A/B, 2014.

[7] A. Hayati-Soloot, Resonant Overvoltages in offshore wind farms-Analysis, modeling and measurement, PhD thesis NTNU, 2017

[8] K. Velitsikakis, C.S. Engelbrecht, K. Jansen, B. van Hulst, “Challenges and Mitigations for the Energization of Large Offshore Grids in the Netherlands”, IPST 2019.

[9] A Holdyk and H Kocewiak, Resonance Characteristics in Offshore Wind Power Plants with 66 kV Collection Grids, J. Phys.: Conf. Ser. 1356 012025, 2019

[10] S. E. Zirka, Y. I. Moroz, N. Chiesa, R. G. Harrison, H. Kr. Høidalen, “Implementation of Inverse Hysteresis Model Into EMTP—Part II: Dynamic Model”, IEEE TRPWD, Vol. 30, Issues 5, pp. 2233-2241, 2015

[11] H. K. Høidalen, A. Lotfi, S. E. Zirka, Y. I. Moroz, N. Chiesa, and B. A. Mork, “Benchmarking of hysteretic elements in topological transformer model”, IPST 2015.

[12] H. K. Høidalen, N. Chiesa, A. Avendaño, B. A. Mork: “Developments in the hybrid transformer model –Core modeling and optimization”, IPST 2011.

[13] M. Salimi, A. M. Gole, R. P. Jayasinghe, « Improvement of Transformer Saturation Modeling for Electromagnetic Transient Programs”, IPST 2013.

[14] DIgSILENT, PowerFactory 2024 Technical References Models.

[15] D. Goldsworthy, T. Roseburg, D. Tziouvaras and J. Pope, "Controlled Switching of HVAC Circuit Breakers: Application Examples and Benefits," 2008 61st Annual Conference for Protective Relay Engineers

[16] Cigre WG A3.07: Controlled switching of HVAC CBs - Planning, specifications & testing, TB264, 2004